



## Synthesis and Characterization Of Dextran Coated Magnetite Nanoparticles Loaded With Curcumin And *In Vitro* Cytotoxicity Study In MCF-7 Cancer Cells.

Omayma Abouzaid<sup>1</sup>, Omama E. El Shawi<sup>2</sup>, Nahla A. Mansour<sup>3</sup>, Aml M. Hanafy<sup>4</sup>

<sup>1</sup>Department of Biochemistry, Faculty of Veterinary Medicine, Benha University

<sup>2</sup>Departement of health & Radiation Research, National Centre for Radiation Research and Technology (NCRRT), Atomic Energy Authority, Cairo Egypt.

<sup>3</sup>Department of Petrochemicals, Petroleum Research Institute, Cairo, Egypt.

<sup>4</sup>specialist medical -lab

### ABSTRACT

Medicinal plants are considered to be bioactives valuable sources of anti-cancer. But these compounds are hydrophobic in nature and thus show decreased bioavailability. To overcome this issue, biocompatible drug delivery agents could be conjugating with these bioactives to improve their therapeutic efficacy. In the present study Curcumin loaded dextran coated Fe<sub>3</sub>O<sub>4</sub>NPs was synthesized by chemical precipitation method and coated with Dextran (DEX) using diffusion method. The structural, morphological and the magnetic properties of the prepared materials were studied by using Fourier transform infrared (FT-IR) spectroscopy, transmission electron microscopy (TEM), X-ray diffraction (XRD), dynamic light scattering (DLS), zeta potential and Vibrating Sample Magnetometer (VSM). The MTT (3-(4,5-dimethylthiazol-2-yl)-2,5-diphenyl tetrazolium) assay of CUR loaded dextran coated magnetite nanoparticles (CUR/DEX/Fe<sub>3</sub>O<sub>4</sub>)NPs exhibited notable toxicity against MCF7 cells in a dose and time dependant manner. The IC<sub>50</sub> values were 177µg/ml and 109µg/ml after 24h and 48h incubation respectively.

**Keywords:** Curcumin, Dextran, Fe<sub>3</sub>O<sub>4</sub>, nanoformulation/ anticancer

(<http://www.bvmj.bu.edu.eg>(BVMJ-33(2): 365-374, 2017)

### 1. INTRODUCTION

Conventional therapies of cancer cause serious side effects, systemic toxicity, poor quality of life of patients, accompanied with tumor resistance and recurrence which discourage their long term use. Therefore, highly precise anticancer therapies with minimal side effects are needed to be identified as curcumin, which have been shown to suppress and/or prevent cancer (Yinn et al., 2013, Ahmed et al., 2013).

However, most of these bioactive compounds are hydrophobic in nature and thus show decreased bioavailability (Bhattaram et al., 2002). This could be overcome by conjugating these herbal bioactives with biocompatible drug delivery agents that would improve their therapeutic efficacy (Bhadoriya et al., 2011). Curcumin ((1, 7-bis (4- hydroxy 3-methoxy phenyl)-1, 6-heptadiene-3, 5-dione) is a widely known

natural bioactive polyphenolic component of turmeric safety, widespread availability, low cost, and nontoxicity of curcumin at high doses are well established by human clinical trials (Gupta et al., 2012). So the anticancer activities of curcumin justify its development as a drug for cancer treatment. Preclinical and clinical studies related with oral administration of curcumin have revealed its very poor bioavailability due to its very low aqueous solubility, tendency to degrade in the gastrointestinal tract in the physiological environment, high rate of metabolism, and rapid systemic elimination (Gupta et al., 2013). These issues could be overcome by conjugating these herbal bioactives with biocompatible drug delivery agents that would improve their therapeutic efficacy (Bhadoriya et al., 2011). Dextran, a polysaccharide, has been extensively and successfully used for various in vivo applications. Dextran-coated SPIONs provide desirable stability with no reported toxicity and also provide a powerful nanoparticles platform for the targeted delivery of therapeutics (Zhang et al., 2012). A therapeutic superparamagnetic iron oxide nanoparticles (SPION) typically consists of three primary components: an iron oxide nanoparticles core that serves as both a carrier for therapeutics and contrast agent for MRI, a coating (Dextran) on the iron oxide nanoparticles that promotes favorable interactions between the SPION and biological system, and a therapeutic payload that performs designated function in vivo (Kievit and Zhang, 2011). Collectively, and based on the aforementioned, the present study was undertaken to prepare dextran coated iron oxide nanoparticles (DEX/Fe<sub>3</sub>O<sub>4</sub>) NPs and then payload with Curcumin to obtain CUR/DEX/Fe<sub>3</sub>O<sub>4</sub>-NPs. The formulated Nanosystem was characterized with different techniques. Then

its cytotoxic potential was evaluated in vitro against MCF-7 human breast cancer cell lines.

## 2. Materials and methods

Curcumin 95% (total curcuminoid content), and used as received was purchased from Alfa Aesar, Thermo Fisher Scientific, Shore Road, Port of Heysham Industrial Park, Heysham, Lancashire LA3 2XY, United Kingdom. All other chemicals were obtained from Sigma Aldrich (St. Louis, MO), Merck (Darmstadt, Germany).

### 2.1. Preparation of magnetic nanoparticles:

The magnetic NPs were prepared by controlled chemical coprecipitation of the magnetite phase from aqueous solutions containing suitable salts of Fe<sup>2+</sup> and Fe<sup>3+</sup> under an inert atmosphere according to the procedure conducted by Gupta & Gupta (2005).

### 2.2. Synthesis of dextran coated magnetite (Fe<sub>3</sub>O<sub>4</sub>) nanoparticles:

Based on the method reported previously (Anastasia, et al 2015) dextran coated magnetite (Fe<sub>3</sub>O<sub>4</sub>) nanoparticles were prepared.

### 2.3. Preparation of curcumin-loaded dextran coated MNPs:

Curcumin-loaded dextran coated MNPs were synthesized according to the method reported by Khalkhali, et al (2015).

### 2.4. Characterization

#### 2.4.1. Fourier Transform Infrared spectroscopy analysis.

The spectra were registered on the spectrometer model type Mattson-Infinity Series Benchtop 961 have been employed, one milligram of each sample of raw and modified alumina silicate was ground and specified with a resolution of 2 cm<sup>-1</sup> in the range of 4000-400 cm<sup>-1</sup>.

#### 2.4.2. Particle size and zeta potential.

The particle size distributions were measured with Malvern Zeta Sizer nano series (NANO-ZS) HT using dynamic light scattering in ethanol.

#### 2.4.3. Wide angle X-ray diffraction.

WAXD styles were registered with a Pan Analytical Model X-Pert Pro, which was connected with CuK $\alpha$  radiation ( $\lambda = 0.1542$

nm), Ni-filter and a general area detector. The diffractograms were recorded in the  $2\theta$  range of  $10 - 80^\circ$  with a step size of  $0.02^\circ$  and a step time of 0.7000 s, with generator settings 40 MA, 40 kV.

#### 2.4.4. High resolution transmission electron microscopy.

Images of the nanocomposite were recorded using a JEM-2100F (JEOL) at an acceleration voltage of 200 kv. A few drops of nanocomposite solution were diluted into 1 ml of ethanol, and the resulting ethanol solution was placed onto a carbon coated copper grid and allowed to evaporate.

#### 2.4.5. Vibrating Sample Magnetometer (VSM)

Magnetic measurements were executed with the Quantum Design Model 6000 and parameters such as ( $M_s$ ), ( $H_c$ ) and ( $M_r$ ) were evaluated.

In-vitro cytotoxicity of (CUR/DEX/Fe<sub>3</sub>O<sub>4</sub>) NPs in MCF-7 cells:

The cytotoxicity of CUR/DEX/Fe<sub>3</sub>O<sub>4</sub> NPs was evaluated by MTT (3-(4,5-dimethylthiazol-2-yl)-2,5-diphenyl tetrazolium) assay using the previously reported method (Hansen et al, 1989).

### 3. RESULTS

#### 3.1. Fourier transforms infrared spectroscopy (FTIR)

The FT-IR spectra were recorded to prove the successful preparation of samples and possible interaction between various constituents of nanoparticles. FT-IR spectrum of the MNPs (MNPs), dextran (DEX), dextran coated MNPs (MNP-DEX), free curcumin (CUR), and curcumin loaded dextran coated MNPs (MNP-DEX-CUR) are shown in Fig. 1. FT-IR spectrum of MNPs exhibits the band at  $580\text{ cm}^{-1}$  which is assignable to the absorption of  $\nu$  (Fe–O), and the broad absorption peak appeared at about  $3407\text{ cm}^{-1}$  can be related to the presence of hydroxyl groups. Comparing spectra (MNPs) and (MNP-DEX), some new absorption bands are

appeared. For instance, the bands at about  $1030$ ,  $1007$ , and  $1158\text{ cm}^{-1}$  were due to the stretching vibration of the alcoholic hydroxyl (C–O), and the band at  $1405\text{ cm}^{-1}$  was attributed to the bending vibration of C–H bond. These data proved that the surface of MNPs has been covered with dextran polymer (Banerjee et al., 2007, Hong et al., 2008). It is believed that different interactions such as van der Waals force, hydrogen bond, and electrostatic interactions keep dextran on the surface of MNPs.

As shown in Fig. 1 (spectrum CUR), the FT-IR results exhibit the broad absorption band at  $3430\text{ cm}^{-1}$  indicating the presence of phenolic O–H group. Furthermore, an absorption band at  $1630\text{ cm}^{-1}$  attributed to stretching vibrations of benzene ring, absorption peak at  $1510\text{ cm}^{-1}$  imputed to C=O, band at  $1428\text{ cm}^{-1}$  indicates functional group of olefinic C–H bending vibration and  $1277\text{ cm}^{-1}$  can be assigned to the aromatic C–O stretching vibration (Yallapu, et al 2010). By comparing spectra CUR and MNP-DEX-CUR, the characteristic peaks of curcumin in curcumin loaded MNPs are distinguishable even though the main region of spectra is overlapped. In other words, it clearly demonstrated that curcumin was successfully entrapped in dextran coated MNPs. 3.2. X-ray diffraction analysis

The crystalline nature and phase analysis for the pristine of MNPs, MNP-DEX and MNP-DEX-CUR, has been confirmed by XRD analysis as shown in (Fig. 2). It was clear that there were six diffraction peaks corresponding to six faces of (220), (311), (400), (422), (511) and (440) which were characteristic for single phase spinel structure of Fe<sub>3</sub>O<sub>4</sub>. All the diffraction peaks were very well matches with cubic inverse spinel structure of magnetite nanoparticles. The FWHM of the major diffraction peak (311) was used to calculate the average particle

size. The estimated average particle sizes using Scherrer formula (Li et al., 2004) were  $D = 0.9 \lambda / \beta \cos \theta$  where  $\lambda$  is wave length of X-ray (0.1541 nm),  $\beta$  is FWHM (full width at half maximum),  $\theta$  is the diffraction angle and 'D' is particle diameter size. For the pristine, dextran coated and dextran-curcumin magnetite nanoparticles were 17.7, 11.95 and 21.26 nm respectively. The small decrease in the intensities of the diffraction peak for the dextran coated nanoparticles as shown in (Fig. 2) may be due to the in-situ addition of dextran on the surface of magnetite nanoparticles and it also significantly reduces the average crystalline size. No other extra peaks were observed in the XRD pattern confirms the high purity of the magnetite nanoparticles (Kumar et al., 2014).

Figure 3 shows the magnetization curves of the naked MNPs, dextran-curcumin coated MNPs. The results showed that the samples exhibited superparamagnetic properties. The saturation magnetization values ( $M_s$ ) of the MNPs and MNP-DUX-CUR, were 61.145 and 49.945 emu/g, respectively. As shown in Fig. 5, the decrease in the saturation magnetization of the samples may be due to the effect of higher density of polymer (dextran) on the surface of magnetite nanoparticles. This polymer molecule produces magnetic dead layer on the surface of the magnetite nanoparticles that quenches the surface magnetic moments (Aslibeiki et al., 2012). It was shown that the thickness of shell was determinant parameter in the extent of magnetization decrease.

### 3.3. Morphology and size distribution analysis

The morphology and size of the MNPs were obtained by recording the transmission electron microscopic images. The obtained microscopic image for the pristine Fe<sub>3</sub>O<sub>4</sub> nanoparticles in (Fig. 4) shows spherical aggregates with smooth surface in the size less than 8 nm. These spherical aggregates

were obtained due to the absence of driving force in the surface of the particles or more plausible due to the inter-particle interaction (Chang et al., 2012). The distance between the two particles was below 10 nm and the particles would form an aggregate (Kumar et al., 2010). It confirms the final nanoparticles were prone to get aggregated due to strong magnetic dipole-dipole interaction without using surfactant.

The size of MNPs before and after surface modification was investigated by DLS analysis. In the case of naked MNPs, the size of nanoparticles was about 193 nm (Fig. 5a). The particle size distribution curves exhibited only one peak with a relative high polydispersity index indicating the MNPs aggregation in solution. The size of dextran coated MNPs was also analyzed by DLS. The results showed that the particle size of dextran coated MNPs decreased to 90 nm (Fig. 5b). Decrease in particle size after dextran coating can be related to the impact of dextran coating on protecting MNPs from aggregation which consequently results in high dispersion capability of MNPs. While the particle size of curcumin-dextran coated MNPs is 76 nm (figure 5c).

Zeta potential measurement evaluates the surface charge of nanoparticles and can be indicative of the extent of their stability. For MNPs and dextran coated MNPs, the zeta potential value was obtained to be -0.896 and -23.1 mV, respectively. Apparently, coating MNPs with dextran caused a significant decrease in zeta potential (figures. 5a and 5b). It is believed that the negative value of zeta potential for MNPs arises from the existence of OH<sup>-</sup> groups on the surface of MNPs. Thereby, reduction in surface charge after dextran coating can be evidence of hydrogen bonding between the O- groups of dextran and hydroxyl group of MNPs. zeta potential measurement for MNP-DEX-CUR -21.2 mV

(figures. 5c), from these results it is clear that the negative value of zeta potential for MNPs decreased due to addition of curcumin to dextran magnetic nanoparticles.

### 3.4. Biological *in vitro* results

It is imperative to assess the cytotoxicity of our developed CUR/DEX/Fe<sub>3</sub>O<sub>4</sub> for its potential anticancer application. The evaluation of cytotoxic activity was performed by MTT assay after incubation for 24h (table 1) as well as for 48h (table 2).The

results showed that the viability of MCF-7 cancer cells decreased in a concentration and time dependent manner. The IC<sub>50</sub> values were 177.4µg/ml and 109.7µg/ml after incubation for 24h and 48h respectively.

Table (1):Data expressed as the mean±SD of three separate experiments, \*P is the statistic significant compared to control set.

Concentration of the drug (µg/ml)	Treatments			IC50
	Control	CUR/DEX/Fe <sub>3</sub> O <sub>4</sub> NPS treated cells		
	Cell viability	Cell viability	*P value	
6.25	248.2±8.3	96.5±4.7	0.0001	177.4±4.9
12.5	240.1±9.8	86.6±5.7		
25	238.3±10.3	81.8±4.8		
50	232.9±7.7	77.8±4.9		
100	191.2.5±2.1	64.4±1.6		

Table (2): Data expressed as the mean±SD of three separate experiments, \*P is the statistic significant compared to control set.

Concentration of the drug (µg/ml)	Treatments			IC50
	Control	NARNPS treated cells		
	Cell viability	Cell viability	P value	
6.25	208.9±3.3	109.8±9.2	0.0001	109.7±4.9
12.5	201.8±2.8	98.6±5.7		
25	188.7±4.3	83.1±2.1		
50	179.9±1.7	74.1±6.5		
100	177.7±1.3	61.9±3.5		

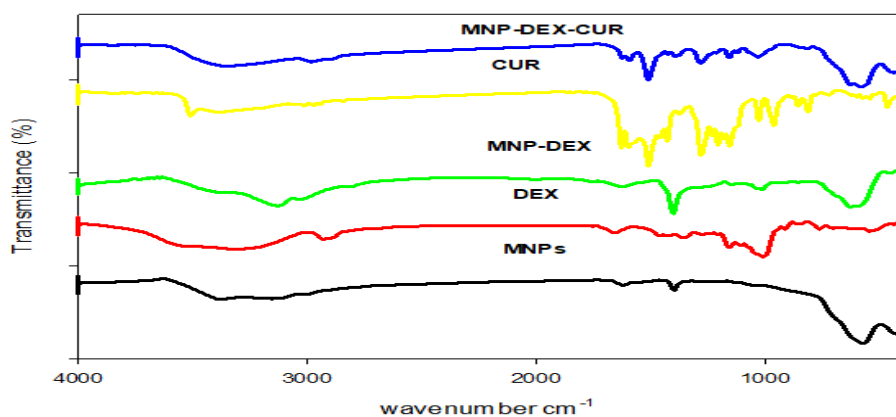


Fig1.FT-IR spectra of MNPs, dextran (DEX), dextran coated MNPs (MNP-DEX), free curcumin (CUR), and curcumin loaded dextran coated MNPs (MNP-DEX-CUR).

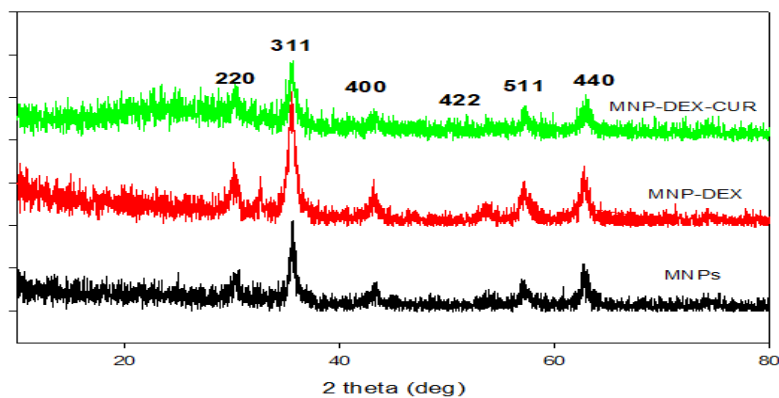


Fig 2. XRD pattern for the MNPs,(MNP-DEX) and (MNP-DEX-CUR)Magnetic properties

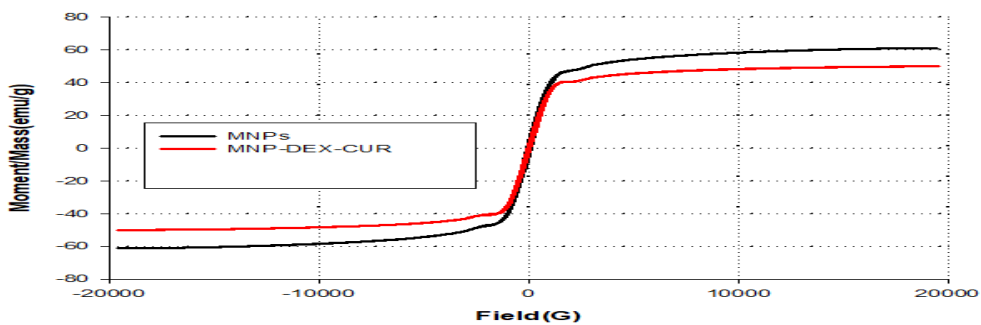


Fig. 3Magnetization vs. applied magnetic field of MNPs and MNP-DEX-CUR

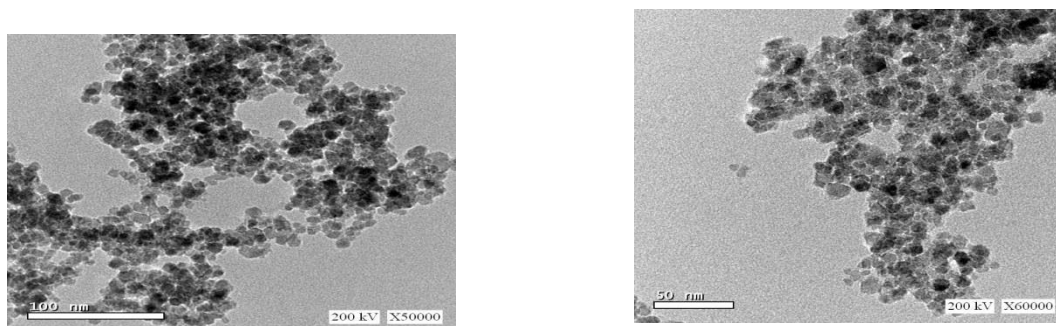


Fig. 4 The viability of MCF-7 cancer cells after 48 hour incubation in CUR/DEX/Fe3O4 compared to control untreated cells: Morpholgy and size di

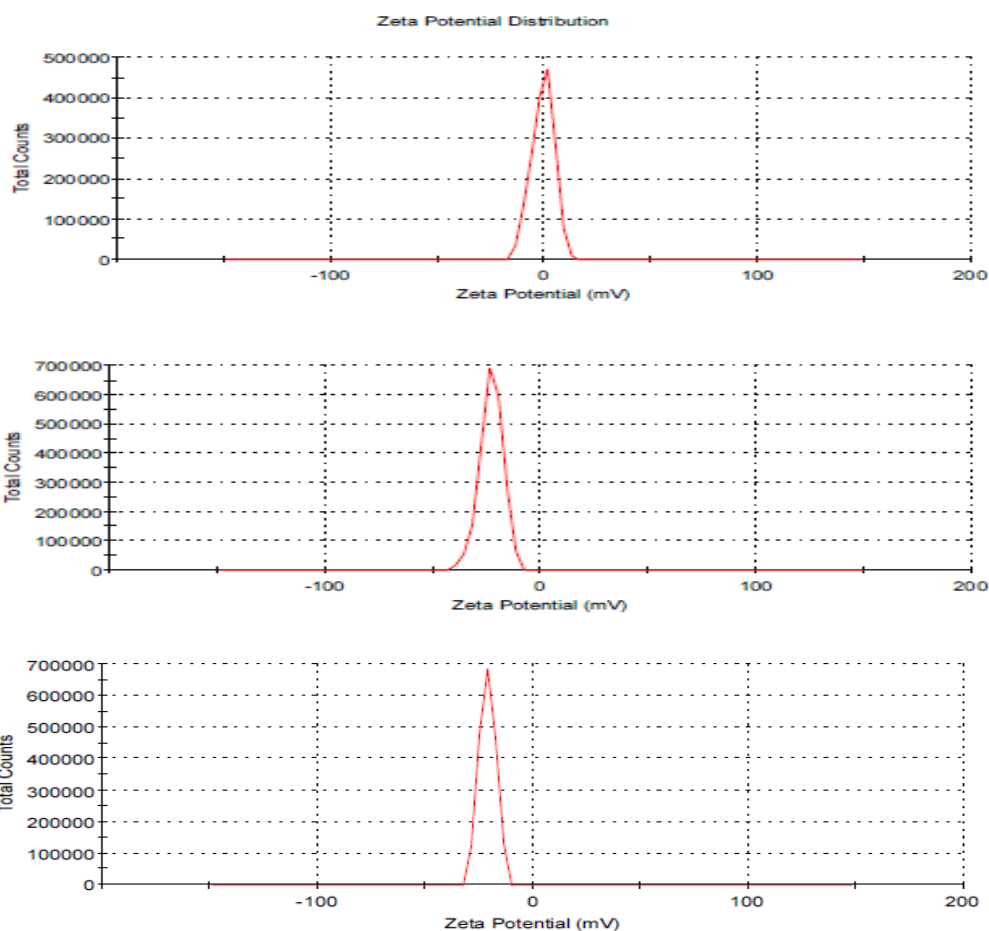


Fig.5a) zeta potential and DLS particle size distribution of MNPs. b) zeta potential and DLS particle size distribution of dextran coated MNPs. c) zeta potential and DLS particle size distribution of curcumin dextran coated MNPs.

#### 4. DISCUSSION

The present study was designed for synthesis of CUR NPs using magnetite ( $\text{Fe}_3\text{O}_4$ ) NPs which used as the core and biocompatible component enhancing the efficacy of the encapsulation of curcumin. In a drug carrier system, the sizes, surface properties, and stability are the crucial features. Partially, the IONPs should be small enough to penetrate through the capillary bed. However, if the diameter of the IONPs is smaller than 10 nm, they will be rapidly removed through extravasations and renal clearance. In the current work, the prepared CUR/DEX/ $\text{Fe}_3\text{O}_4$ NPs Previous reports evidenced that NPs with diameter ranging

from 10 to 100 nm are optimal for intravenous injection and have the most prolonged blood circulation times (Laurent et al .,2008). Dextran caused fictionalization of the MNPs, Zhu and colleagues reported that dextran functionalized MNPs to enhance its capability as drug delivery agent because of the hydrophobic nature of MNPs surface which lead to easily absorption at the protein surface and result in low circulation time (Zhu et al ., 2012).The in vitro cytotoxicity study displayed that our developed nanocurcumin exhibited antiproliferative effect in MCF-7 cancer cells, however significantly reduced the cell viability compared to control untreated cells at a dose and time dependentmanner (tables 1& 2).Previous

studies have reported that magnetic IONP-based drug targeting is a promising cancer treatment method for avoiding the side effects of conventional chemotherapy by reducing the systemic distribution of drugs and lowering the doses of cytotoxic compounds (Cao et al., 2008). Other researchers indicated that nano particulate drug carriers with a diameter of 10-100nm are a drug loaded particulates prepared by a natural polymer as a carrier that provide more surface area and have the potential to increase solubility, enhance bioavailability, improve controlled release and enable the precision targeting of the entrapped compound to a greater extent. As a consequence of improved stability and targeting extent, the amount of the drug required to exert specific effect is much less than the amount of encapsulated sample (Saraf, 2010, Liu et al., 2008). Bisht and coworkers manifested that, unlike curcumin, nanocurcumin is freely desirable in water in absence of any surfactants (Bisht et al., 2007). They concluded that Nanocurcumin revealed therapeutic efficacy *in vitro* against various human pancreatic tumor cells, confirmed by cell viability and clonogenic assays. The underlying mechanism of action was as follows: free curcumin was released, inducing apoptosis, blocking the activation of nuclear factor kappa B (NFkB) and regulating levels of pro-inflammatory cytokines, such as interleukin 6, interleukin 8, and the tumor necrosis factor (Bisht et al., 2007). Several studies demonstrated that nanocurcumin enhances bioavailability of curcumin in animals as well as in humans (Guzman-Villanueva, et al., 2013, Zhongfa et al., 2012). Moreover, the sustained-release CUR nanoformulations offer improved availability and reduce the required dose of CUR for cancer therapy. For instance, cyclodextrin (CD), cyclic polysaccharide has improved *in vitro* and *in vivo* bioavailability and

chemotherapeutic efficacy compared to curcumin alone (Yadav et al., 2010).

## 5. CONCLUSION

Curcumin was chosen as a potent anticancer drug and it was loaded on dextran coated magnetite nanoparticles by chemical precipitation method. The successful synthesis of nanocurcumin was confirmed by FTIR analysis. The uniform size, shape, and surface properties of the Curcumin loaded magnetite nanoparticles significantly enhance the anticancer activity in breast cancer cells. Therefore based on the results of the present study, we could conclude that magnetite nanoparticles loaded drug may be an effective approach to deliver an anticancer drug to the targeted cancer cells and also enhances the possible usage in biological applications.

## 6. REFERENCES

- Ahmed, M. Khan, M.I. Khan, M.R., Muhammad, N. and Khan, A.U. 2013. Role of medicinal plants in oxidative stress and cancer. *Open Access Scientific Reports* 2: 641.
- Anastasia, K. H., Ronita, M., Kimberly, W., and Anderson, J. Z. 2015. Hilt The effects of synthesis method on the physical and chemical properties of dextran coated iron oxide nanoparticles *Materials Chemistry and Physics* 160 177e186.
- Aslibeiki, B., Kameli, P., Manouchehri, I., and Salamati, H. 2012. Strongly interacting superspins in Fe<sub>3</sub>O<sub>4</sub> nanoparticles. *Curr. Appl. Phys.*, 12pp 812-816
- Banerjee, S.S. and Chen, D.H. 2007. Fast removal of copper ions by gum arabic modified magnetic nano-adsorbent.

- Journal of Hazardous Materials* 147: 792-9.
- Bhadoriya, S.S., Mangal, A., Madoriya, N., and Dixit, P. 2011. Bioavailability and bioactivity enhancement of herbal drugs by "Nanotechnology": a review. *JCPR* 8: 1-7.
- Bhattaram, V.A., Graefe, U., Kohlert, C., Veit, M. and, Derendorf, H. 2002. Pharmacokinetics and bioavailability of herbal medicinal products. *Phytomedicine* 9: 1-33.
- Bisht, S., Feldmann, G., Soni, S., Ravi, R., Karikar, C., and Maitra A 2007. Polymeric nanoparticle-encapsulated curcumin ("nanocurcumin"): a novel strategy for human cancer therapy. *J Nanobiotechnology*. Apr 17; 5:3.
- Cao, S. W., Zhu, Y. J., Ma, M .Y, Li, L. and Zhang, L. 2008. Hierarchically nanostructured magnetic hollow spheres of Fe<sub>3</sub>O<sub>4</sub> and gamma-Fe<sub>2</sub>O<sub>3</sub>: preparation and potential application in drug delivery *J. Phys. Chem. C* 112 1851
- Chang, B., Zhang ,X., Guo, J., Sun ,Y., Tang, H., Ren, Q., and Yang, W. 2012. General one-pot strategy to prepare multifunctional nanocomposites with hydrophilic colloidal nanoparticles core/mesoporous silica shell structure .*J Colloid Interface Sci.* Jul 1; 377(1):64-75.
- Gupta, A.K., Gupta, M. 2005. Synthesis and surface engineering of iron oxid nanoparticles for biomedical applications. *Biomaterials* 26, 3995-4021.
- Gupta, S.C., Patchva, S., Koh, W., Aggarwal, B.B. 2012. Discovery of curcumin, a component of golden spice, and its miraculous biological activities. *ClinExpPharmacol Physiol.* Mar; 39(3):283-99.
- Gupta, S. C., Sridevi, P. and Bharat B. A. 2013. Therapeutic Roles of Curcumin: Lessons Learned from Clinical Trials. *AAPS J.* Jan; 15(1): 195-218.
- Guzman, V. D., El-Sherbiny, I.M., Herrera, R. D., and Smyth, H.D. 2013. Design and in vitro evaluation of a new nanomicroparticulate system for enhanced aqueous-phase solubility of curcumin. *Biomed Res Int.*; 724-763.
- Hansen, M.B., Nielsen, S.E. and Berg, K. 1989. Re-examination and further development of a precise and rapid dye method for measuring cell growth/cell kill. *J. Immunol. Methods*; 119:203-10.
- Hong, R., Feng, B., Chen, L., Liu, G., Li, H., and Zheng, Y. 2008. Synthesis, characterization and MRI application of dextran-coated Fe<sub>3</sub>O<sub>4</sub> magnetic nanoparticles. *Biochemical Engineering Journal*; 42: 290-300.
- Khalkhali, M., Somayeh, S., Kobra, R., Farhad, K., Mehran, N., Nahid, B., Mina H., Mehrdad, H. 2015. Synthesis and characterization of dextran coated magnetite nanoparticles for diagnostics and therapy Khalkhali et al., *BioImpacts*, 5(3), 141-150.
- Kievit, F.M. and Zhang, M. 2011. Surface engineering of iron oxide nanoparticles for targeted cancer therapy. *Acc Chem Res.* Oct 18; 44(10):853-62.
- Kumar, S., Ravikumar, C., Bandyopadhyaya, R., 2010. State of dispersion of magnetic nanoparticles in an aqueous medium: experiments and Monte Carlo

- simulation. *Langmuir*. Dec 7; 26(23):18320-30.
- Kumar, R. S., Priyatharshni, S., Babu, b. D., Mangalaraj, A. C., Viswanathan, A. S., Kannan, B.N. and Ponpandian 2014. Quercetin conjugated superparamagnetic magnetite nanoparticles for in-vitro analysis of breast cancer cell lines for chemotherapy applications. *Journal of Colloid and Interface Science* 436 234–242.
- Laurent, S., Forge, D., Port, M., Roch, A., Robic, C., Elst, L. V. and Muller, R. N. 2008. Magnetic iron oxide nanoparticles: synthesis, stabilization, vectorization, physicochemical characterizations, and biological applications *Chem. Rev.* 108 2064.
- Li, Z., Chen, H., Bao, H.B., Gao, M.Y., (2004) One-pot reaction to synthesize water-soluble magnetite nanocrystals, *Chem. Mater* 16, 1391e1393.
- Liu, M., Li, H., Luo, G., Liu, Q., and Wang, Y. 2008. Pharmacokinetics and biodistribution of surface modification polymeric nanoparticles. *Arch Pharm Res.* Apr;31(4):547-54.
- Saraf, A. S., 2010. Applications of novel drug delivery system for herbal formulations. *Fitoterapia*. Oct; 81(7):680-9.
- Yadav, V.R., Prasad, S., Kannappan, R., Ravindran, J., Chaturvedi, M.M., and Vaahtera, L., 2010. Cyclodextrin-complexed curcumin exhibits anti-inflammatory and antiproliferative activities superior to those of curcumin through higher cellular uptake. *Biochem Pharmacol.*; 80:1021-32.
- Yallapu, M.M., Jaggi, M., and Chauhan, S.C. 2010.  $\beta$ -Cyclodextrin-curcumin self-assembly enhances curcumin delivery in prostate cancer cells. *Colloids and Surfaces B: Biointerfaces*; 79: 113-25.
- Yin, S.Y., Wei, W.C., Jian, F.Y., and Yang, N.S. 2013. Therapeutic applications of herbal medicines for cancer patients. *Evid Based Complement Alternat Med* 2013: 1–15.
- Zhang, C., Wang, W., Liu, T.Y., Wu, H., Guo, P., Wang, Q., Tian, Y. W., and Yuan, Z. 2012. Doxorubicin-loaded glycyrrhetic acid-modified alginate nanoparticles for liver tumor chemotherapy. *Biomaterials*, 33, 2187–2196.
- Zhongfa, L., Chiu, M., Wang, J., Chen, W., Yen, W., Fan-Havard, P., 2012. Enhancement of curcumin oral absorption and pharmacokinetics of curcuminoids and curcumin metabolites in mice. *Cancer Chemother Pharmacol.*; 69: 679-89.
- Zhu, C. L., Liu, L. B., Yang, Q., Lv, F. T., and Wang, S. 2012. Water soluble conjugated polymers for imaging, diagnosis, and therapy *Chem. Rev.* 112